Supporting Information for

Long afterglow epoxidized soybean oil polymer composites with reversible dynamic cross-linking for intelligent coating

Author：Jiaman Hu,[a] Zihao Wang,[a] Minglin Yang,[a] Chuansong Yu,[a] Siyu Li,[a] Yinggang Miao,[b] Xiangqian Quan,[c] Jize Liu*[a] and Shiyang Shao*[a]

[a.] School of Materials Science and Engineering, Hainan University (Haikou, 570228 Hainan, China)

[b.] Shaanxi Key Laboratory of Impact Dynamics and its Engineering Application, School of Aeronautics, Northwestern Polytechnical University, Xi'an 710072, China; Joint International Research Laboratory of Impact Dynamics and its Engineering Applications, School of Aeronautics, Northwestern Polytechnical University, Xi'an 710072, China; National Key Laboratory of Strength and Structural Integrity, Xi'an 710072, China

[C.] Institute of Deep-Sea Science and Engineering, Chinese Academy of Sciences, Sanya 572000, China; Department of Mechanical and Aerospace Engineering and Scripps Institution of Oceanography, University of California San Diego La Jolla, CA 92093, USA

Corresponding authors：ljz@hainanu.edu.cn; ssyang@hainanu.edu.cn

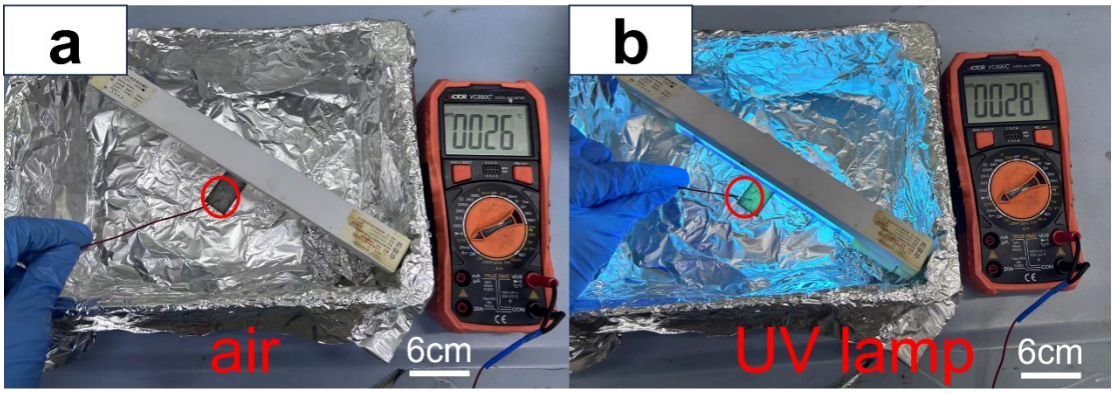

Figure S1. Temperature images of SMT coatings under UV lamp and in air.

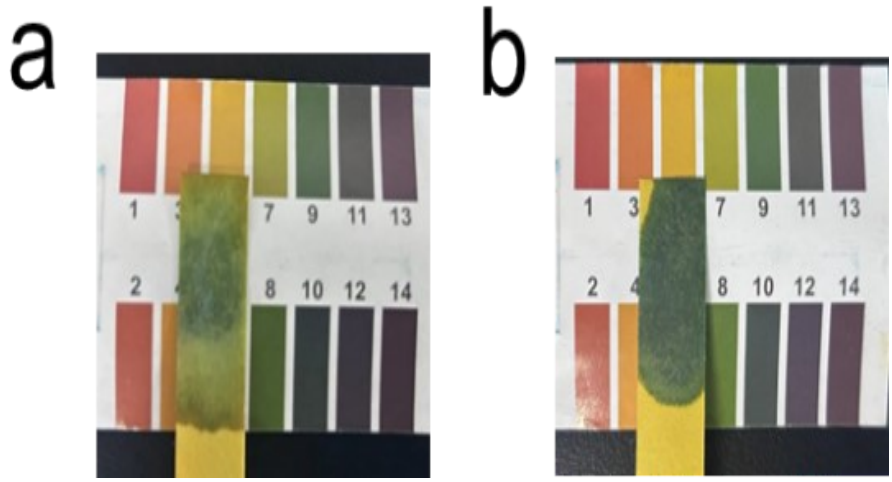

Figure S2. Comparison of PH value of solution of $SrAl_2O_4$: Eu^{2+}, Dy^{3+} powder dissolved in water before and after modification. (a) PH value of modified powder. (b) PH value of unmodified powder solution.

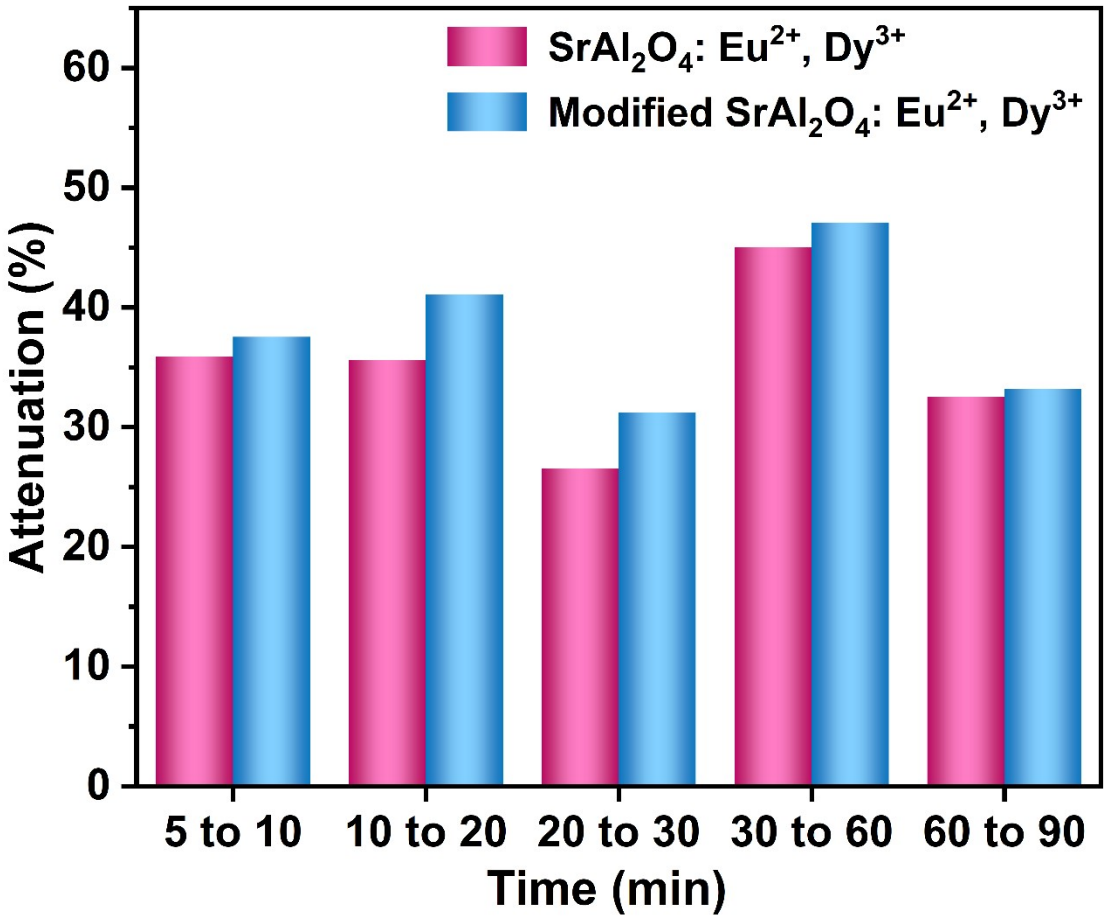

Figure S3. Comparison of PL intensity decay rate before and after powder modification.

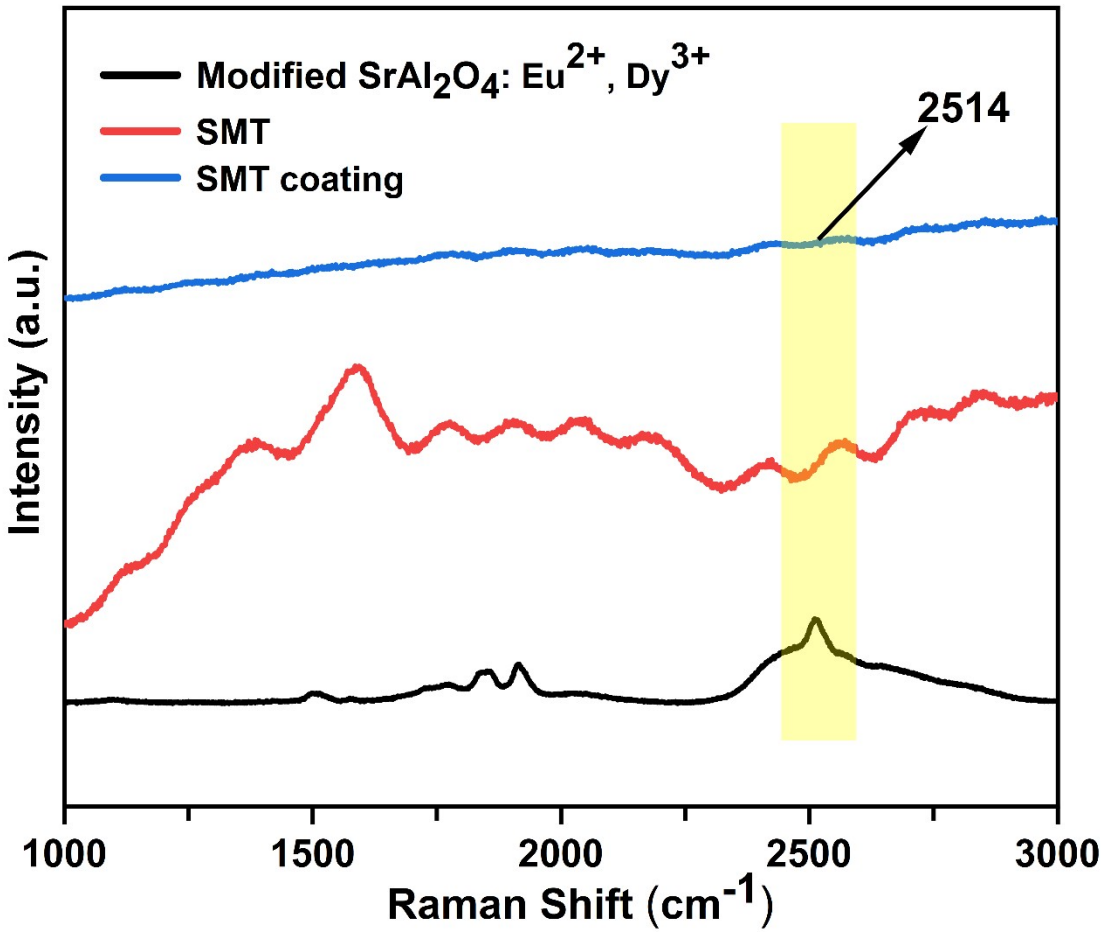

Figure S4. Raman spectra of SMT coatings. The yellow shaded area belongs to the characteristic area of modified $SrAl_2O_4$: Eu^{2+}, Dy^{3+} powder in SMT coatings.

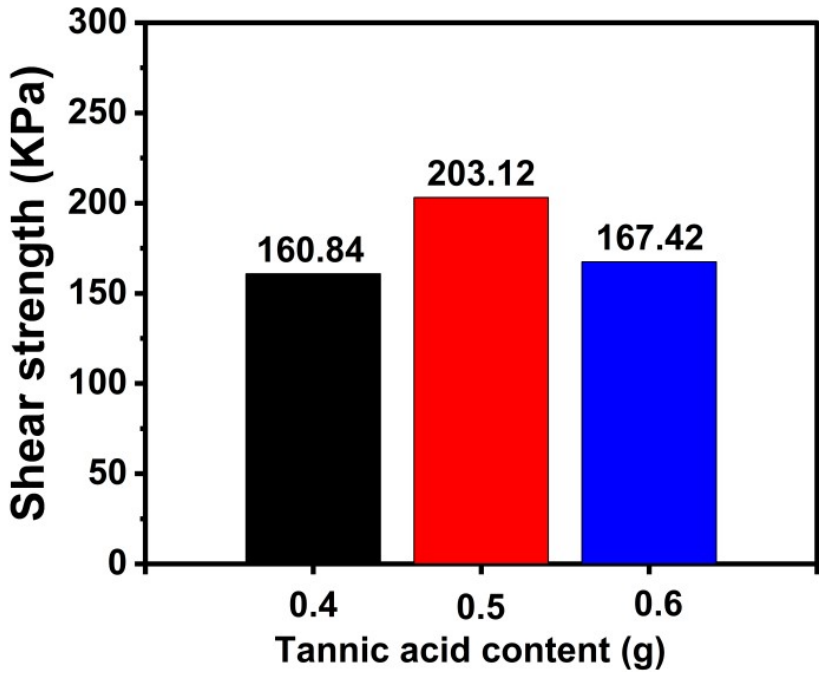

Figure S5. Keeping the content of epoxidized soybean oil and malic acid constant, shear strength of SMT coatings synthesized with different tannic acid (TA) contents at 200mm/min (TA=0.4, 0.5, 0.6g).

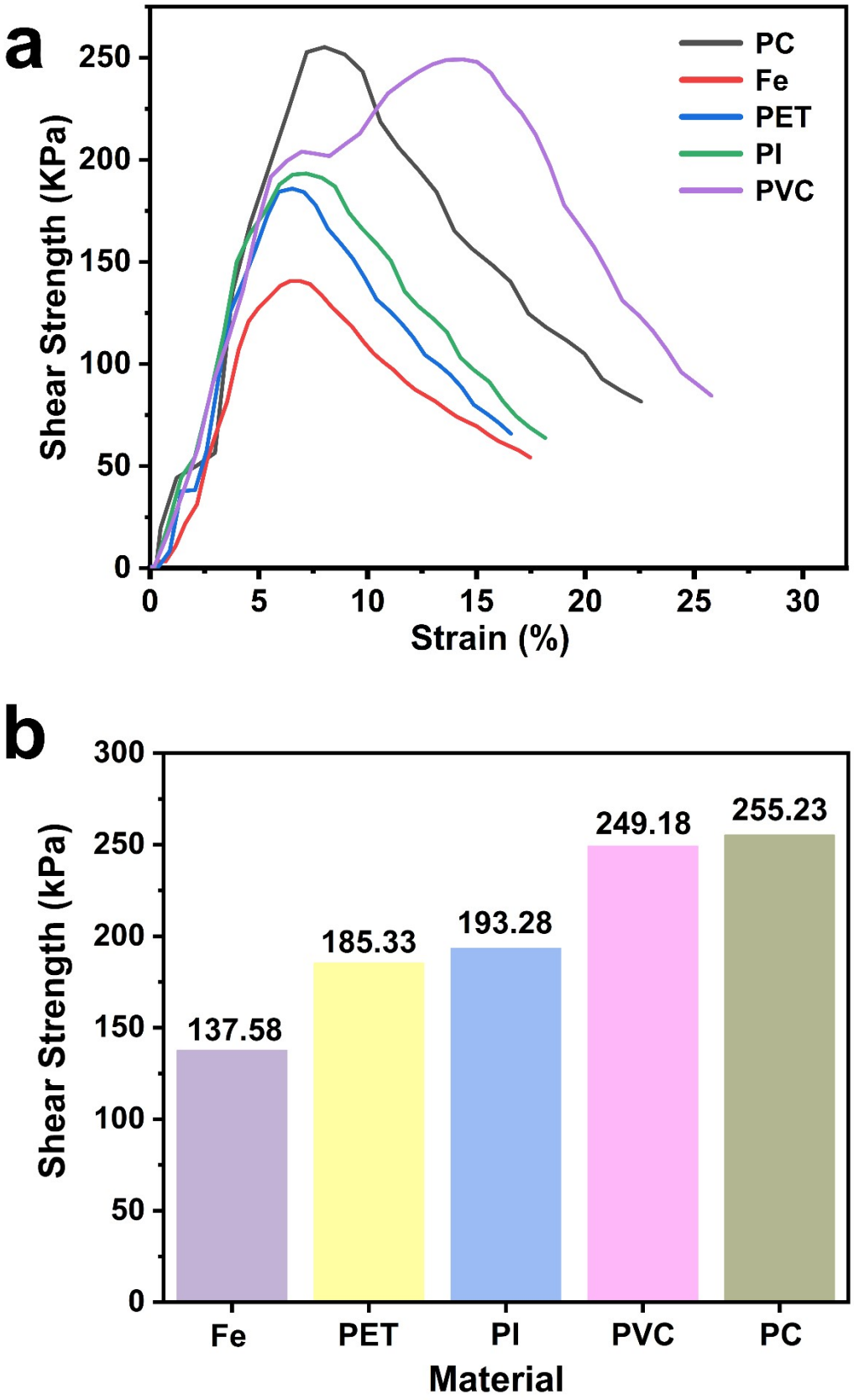

Figure S6. (a) The shear strength-strain curves of SMT coating after self-healing. (b) Shear strength of SMT coatings under different materials.

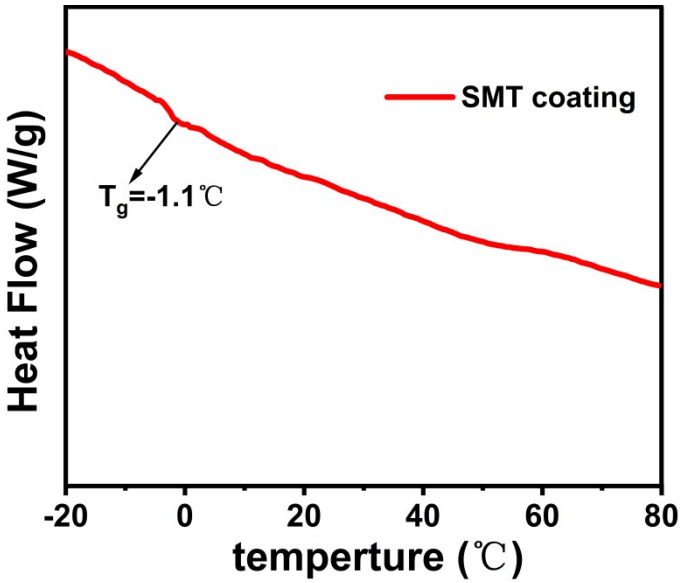

Figure S7. DSC thermograms for SMT coating.

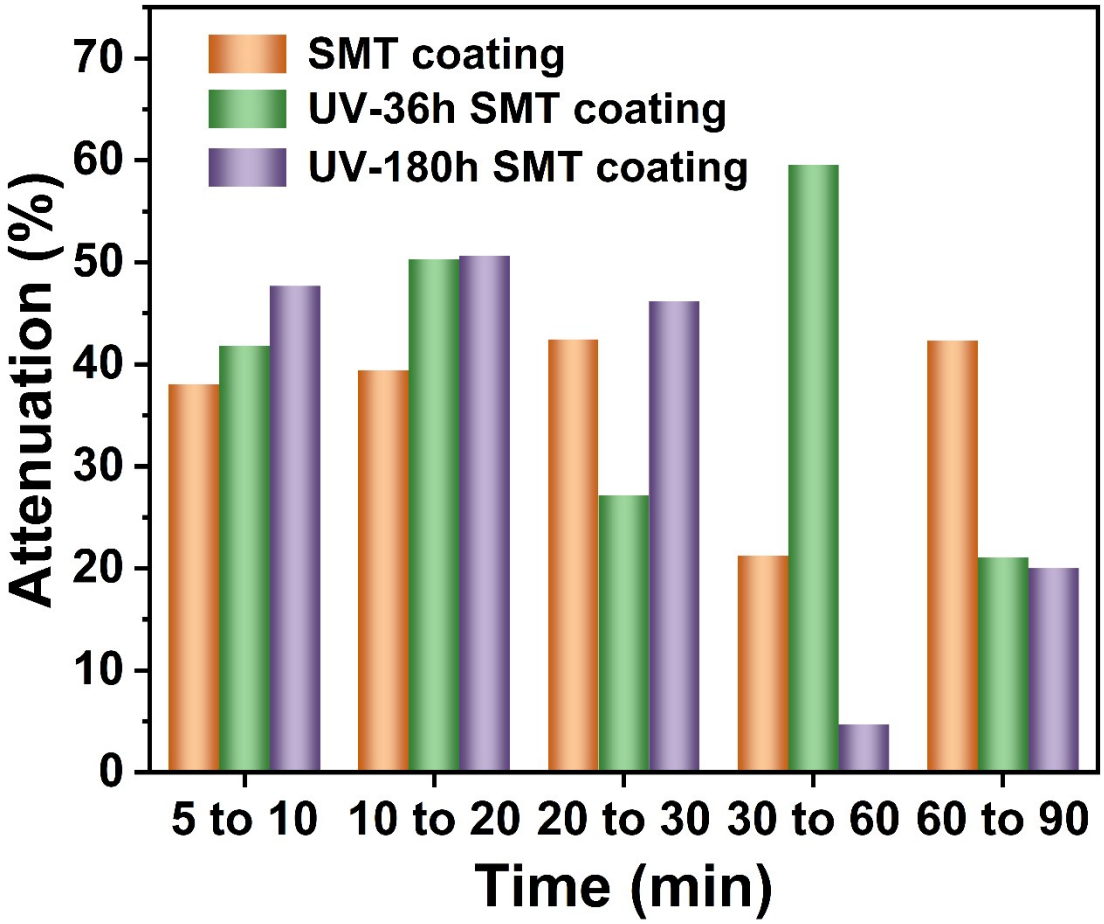

Figure S8. The PL intensity attenuation rates of SMT coating, UV-36 h SMT coating, and UV-108 h SMT coating were compared at different periods.

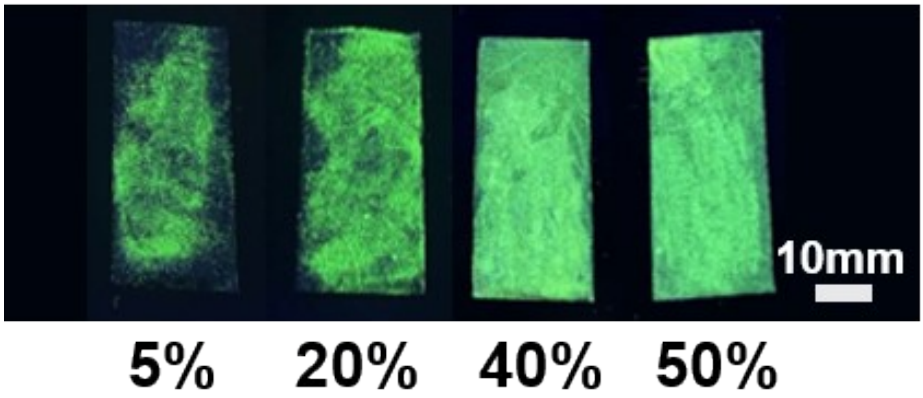

Figure S9. Images of different doping ratios of $SrAl_2O_4$: Eu^{2+}, Dy^{3+} powders mixed with SMT polymers under UV light.

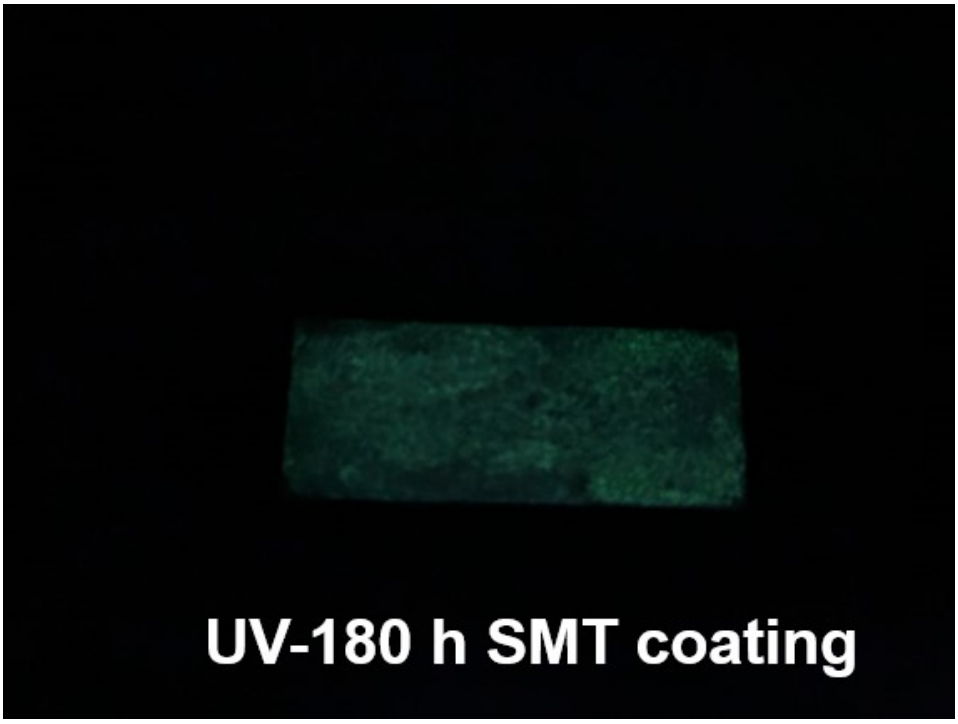

Figure S10. Image of UV-180 h SMT coating under dark conditions.

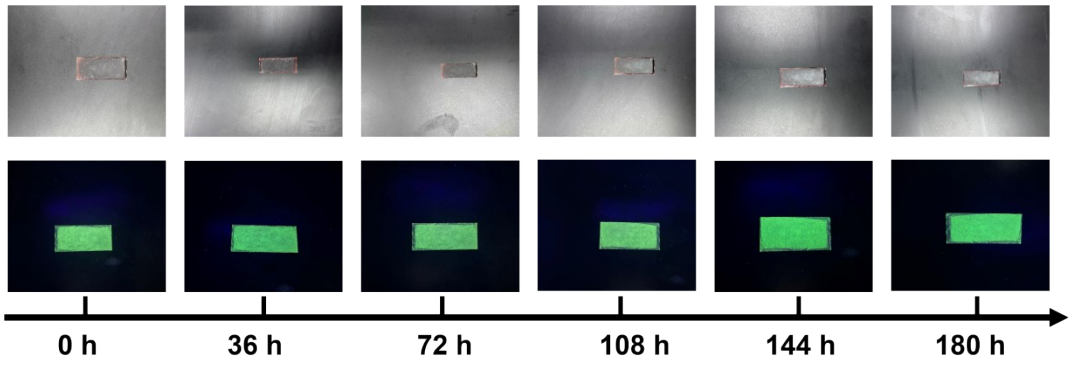

Figure S11 After different cumulative exposure times with UV lamps, image of SMT coating placed in day and irradiated under 365nm UV.

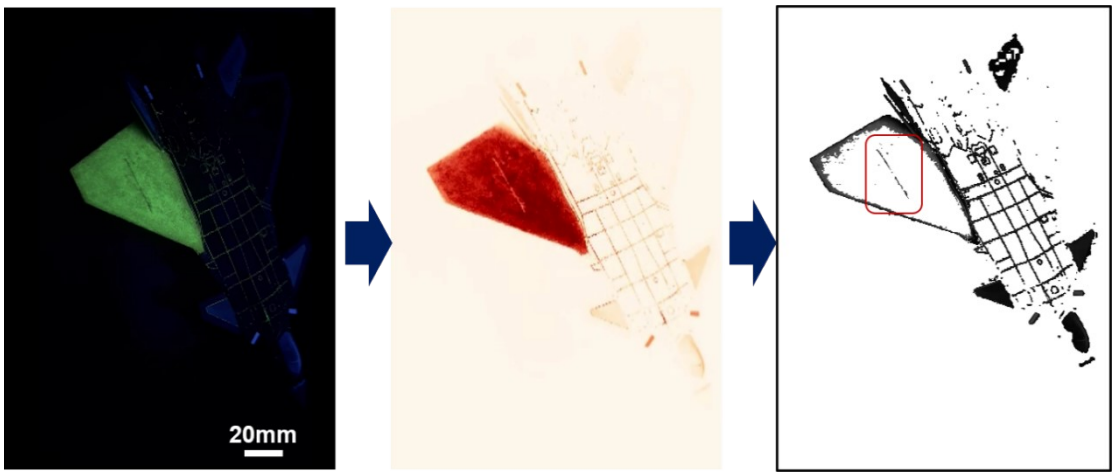

Figure S12. Original digital photo (left), heat map generated based on the green intensity (middle) and boundaries visualization (right) of the aircraft model.

To better analyze the cracks, the captured photos (720*1280) was transformed into digital matrix pixel by pixel, every pixel was quantified as [R, G, B]. After extracting the intensity of green (G value) and generate a heat map, the distribution of green luminescence can be presented in real-time (Movie S2).

Figure S13. Images of SMT coating exposed to air for six months compared with the original coating.

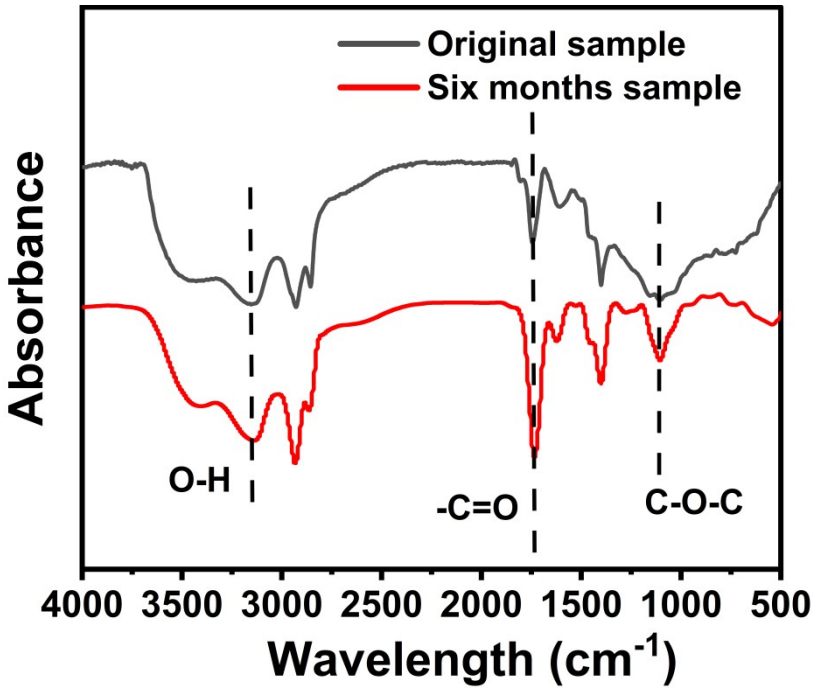

Figure S14. FTIR spectra of SMT coating exposed to air for six months compared with the original coating.

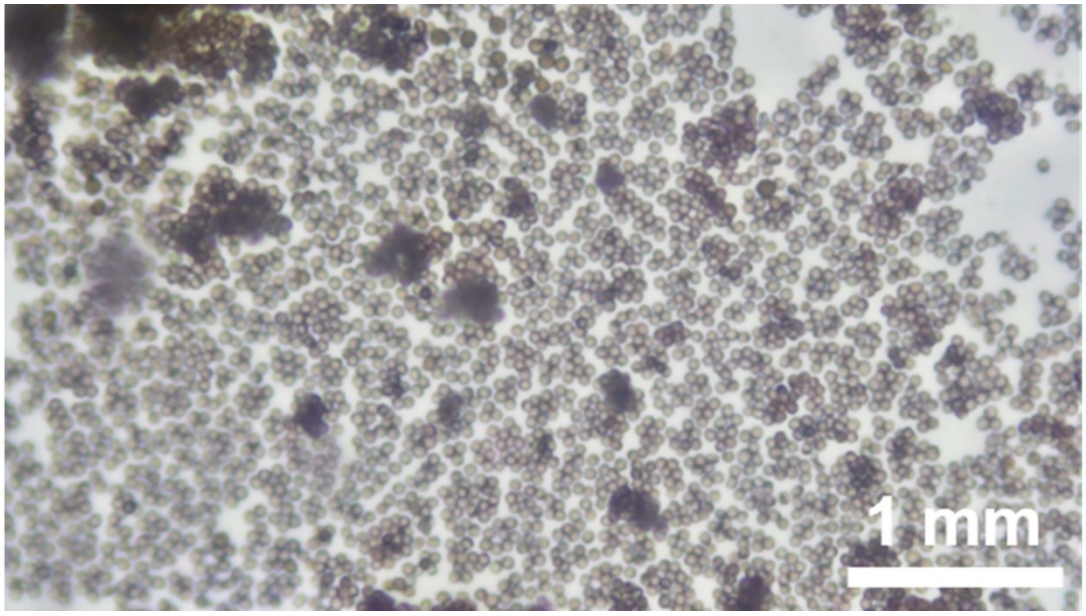

Figure S15. Electron microscope image of colonies during degradation.

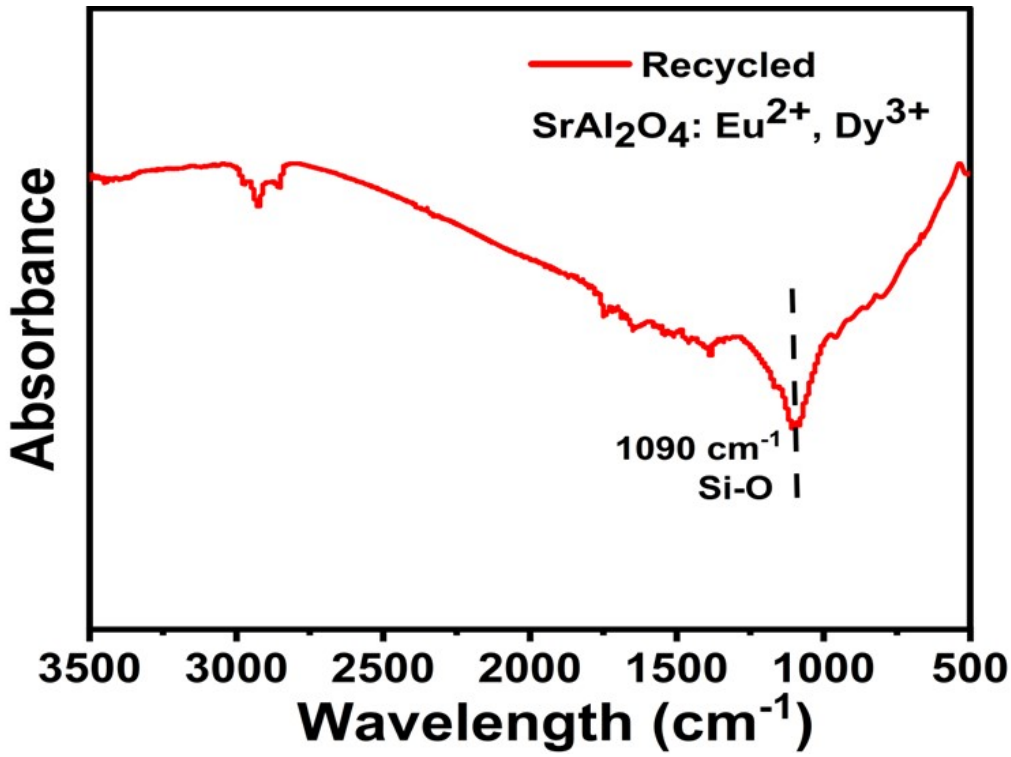

Figure S16. FTIR spectra of the recycled modified $SrAl_2O_4$: Eu^{2+}, Dy^{3+} powder.

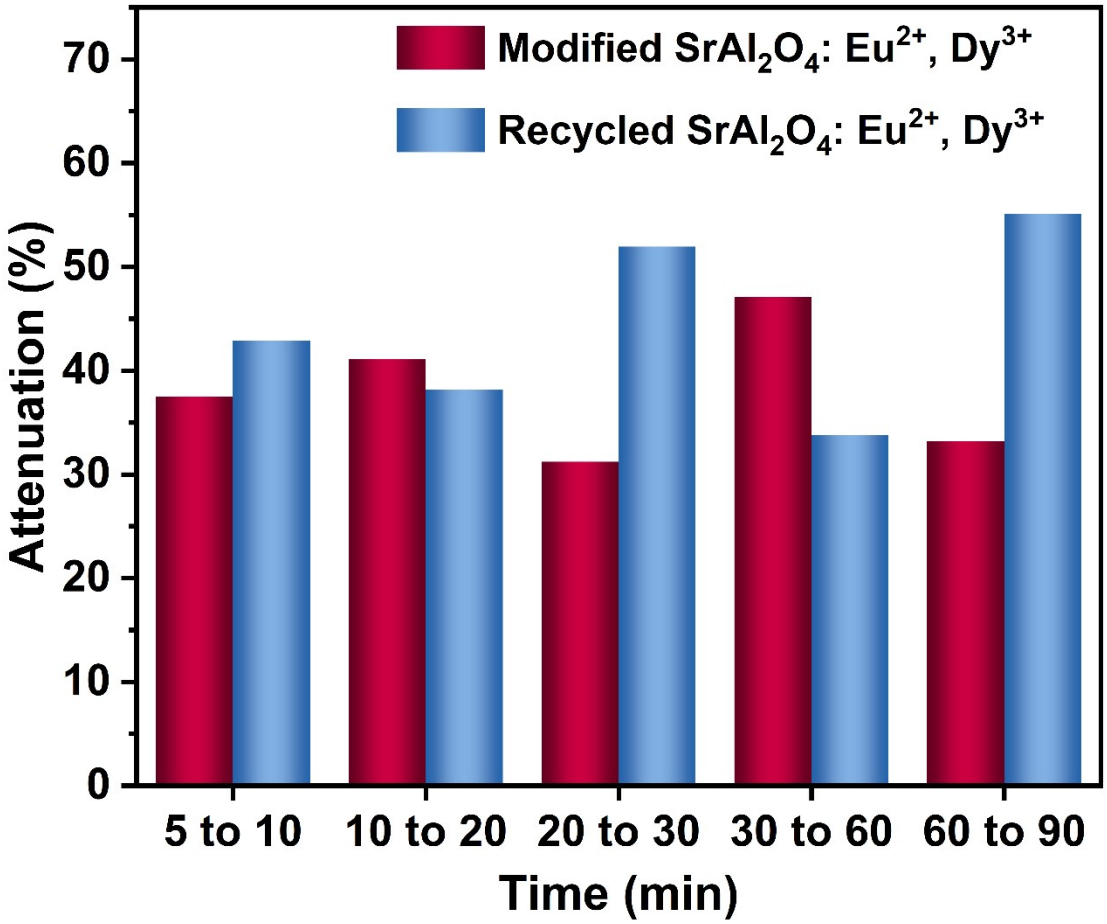

Figure S17. Comparison of PL intensity attenuation rate between recycled powder and modified powder.